# Market-Based Coordinated Planning of Fast Charging Station and Dynamic Wireless Charging System Considering Energy Demand Assignment

Fangzhou Xia, Hongkun Chen, Mingyu Yan, *Member, IEEE*, Wei Gan, *Member, IEEE*, Quan Zhou, *Senior Member, IEEE*, Tong Ding, Xuechun Wang, Lingling Wang, and Lei Chen, *Senior Member, IEEE*



***Abstract*—With the rapid growth of electric vehicle (EV) penetration, EV charging demand is becoming greater and diversified. To meet the diverse EV charging demand, we propose a market-based coordinated planning method of fast charging station (FCS) and dynamic wireless charging system (DWCS). Firstly, a bi-level coordinated planning model considering the benefits of charging service provider and EV user group is built. It can make full use of the complementary characteristics of FCSs and DWCSs. Then, the energy demand assignment(EDA) approach that can directly assign energy demand to roads and power nodes is proposed and applied in the inner level of bi-level coordinated planning model. Finally, the cases that consider the impact of differentiated traffic demand and land prices in different regions are proposed. The case studies are formulated based on the 21 power nodes-12 traffic nodes network and the 54 power nodes-25 traffic nodes network. To calculate the optimal solution, the KKT conditions, the McCormick relaxation approach, the optimization-based bound tightening approach (OBBT) and the sequential bound tightening approach (SBT) are employed. Numerical simulation results validate that the proposed method can effectively improve the profits of charging service provider and keep the EV users' charging cost at relatively low range.**

***Index Terms*—Market-based coordinated planning, fast charging station, dynamic wireless charging system, energy demand assignment, coupled power-traffic networks.**

Manuscript received 15 November 2022; revised 17 March 2023 and 22 June 2023; accepted 24 July 2023. Paper no. TSG-01710-2022. *(Corresponding author: Hongkun Chen.)*

AQ1

Fangzhou Xia, Hongkun Chen, Tong Ding, Xuechun Wang, and Lei Chen are with the School of Electrical Engineering and Automation, Wuhan University, Wuhan 430072, China (e-mail: xiafz92@hotmail.com; chkinsz@163.com; dingtong@whu.edu.cn; wangxuechun@whu.edu.cn; chen_lei@whu.edu.cn).

Mingyu Yan is with the Department of Electrical and Electronic Engineering, Imperial College London, SW7 2AZ London, U.K. (e-mail: mingyu.yan@imperial.ac.uk).

Wei Gan is with the School of Engineering, Cardiff University, CF24 3AA Cardiff, U.K. (e-mail: ganw4@cardiff.ac.uk).

Quan Zhou is with the College of Electrical and Information Engineering, Hunan University, Hunan 410082, China (e-mail: zquan@hnu.edu.cn).

Lingling Wang is with the School of Electronic Information and Electrical Engineering, Shanghai Jiao Tong University, Shanghai 200240, China (e-mail: wanglingling1993@sjtu.edu).

Color versions of one or more figures in this article are available at https://doi.org/10.1109/TSG.2023.3299591.

Digital Object Identifier 10.1109/TSG.2023.3299591

## NOMENCLATURE

*Parameters*

| | |
|---|---|
| $t$, $od$, $k$, $l$ | Index of time segments/O-D pairs/paths /roads |
| $\beta_p$ | Unit penalty cost |
| $T_u$ | Unit time of a time segment |
| $PR_{ic}$, $PR_{id}$ | Upfront costs of each FCS/DWCS |
| $PR_{cp}$, $PR_{dwc}$ | Unit price of FC piles/DWCS (per kilometer) |
| $PR_{pv}$, $PR_{es}$ | Unit price of PVs/ESSs |
| $PR_{dl}$ | Unit price of additional power cables |
| $PR_{MF}$, $PR_{MD}$ | Upper bounds of FC/DWC services prices |
| $PR^t_{pm}$ | Time of use (TOU) electricity price |
| $PR_{opf}$, $PR_{opd}$ | Operating costs per unit time of a single charging pile/ DWCS |
| $PR_{hw}$ | Average hourly wage |
| $PR^l_{ac}$, $PR^l_{av}$, $PR^l_{ae}$ | Land costs of a single set of charging pile/ PV / ESS on road $l$ |
| $\mu_F$, $\mu_D$ | Maximum numbers of FCSs/DWCSs |
| $\mu_P$ | Maximum number of FC piles in any FCS |
| $\mu_V$, $\mu_E$ | Maximum numbers of PVs/ESSs on any road |
| $P^{t,l}_{bl}$, $Q^{t,l}_{bl}$, $S^{t,l}_{bl}$ | Active power/ reactive power/ apparent power of baseload in the corresponding node of road $l$, at time $t$ |
| $P^t_v$ | Maximum output power of a single set of PV at time $t$ |
| $EC^e_{or}$, $EC_{pn}$ | Capacity of a single origin power cable/ additional power cable |
| $EO_l$ | Initial electric quantity of ESSs on road $l$ |
| $\mathrm{EC}_{es}$ | Installation capacity of a single set of ESS |
| $L_l$ | Available length for DWCS on road $l$ |
| $T^{t,l}_d$ | Passing time on road $l$, at time $t$ |
| $P_F$, $P_D$ | Rated charging power of a single FC pile/ single EV charged with DWCS |
| $E^{t,od}_g$ | Energy gap of O-D pair $od$, at time $t$ |
| $\lambda_E$ | Minimum proportion of the energy demand satisfied through FCSs and DWCSs during a typical day |

| | |
|---|---|
| $\eta_{ie}$, $\eta_{oe}$ | Input and output efficiency of ESSs |
| $\eta_F$, $\eta_D$ | Energy transfer efficiency of FC/DWC |
| $\eta_{DWC}$ | The percentage of EVs that support DWC |
| $U_N$ | Nominal voltage of power network nodes |
| $U_m$, $U_M$ | Lower/upper bounds of power network nodal voltage |
| $r_{or}^e$, $x_{or}^e$ | Resistance/ reactance of original cable on power line $e$ |
| $r_{co}^e$, $x_{co}^e$ | Combined resistance/ reactance considering the added power cables on line $e$ |
| $M_{ps}^{t,od,k,l}$ | 1 if path $k$ of O-D pair od includes road $l$, at time $t$; and 0, otherwise |
| $n_r^l$ | Number of lanes in one direction on road $l$ |
| $tv_u$, $tv_l$ | Tolerance values of upper bound/lower bound, in OBBT |
| $tv_s$ | Convergence tolerance in SBT |
| $\varepsilon$ | Local feasible solution of the original bi-level problem |
| $\{\psi^j\}_{j=1}^J$ | Decreasing sequence in SBT |
| $\delta_M$ | Big constant in the big-M approach |

*Variables*

| | |
|---|---|
| $E_f^{t,od,k,l}$ | FC demand of O-D pair od, path $k$, on road $l$, at time $t$ |
| $E_d^{t,od,k,l}$ | DWC demand of O-D pair od, path $k$, on road $l$, at time $t$ |
| $M_{rf}^l$, $M_{rd}^l$ | 1 if FCS/DWCS is built on road $l$; and 0, otherwise |
| $M_{pn}^e$ | 1 if additional power cable is built on power network line $e$; and 0, otherwise |
| $n_{cp}^l$, $n_{pv}^l$, $n_{es}^l$ | Numbers of FC piles/PVs/ESSs installed on road $l$ |
| $PR_F^t$, $PR_D^t$ | FC/DWC service prices at time $t$ |
| $P_{dn}^{t,l}$, $Q_{dn}^{t,l}$ | Active/reactive power from power network to FCS and DWCS on road $l$, at time $t$ |
| $P_{pv}^{t,l}$, $P_{es}^{t,l}$ | Output power of PVs/ESSs on road $l$, at time $t$ |
| $P_{ad}^{t,e}$, $S_{ad}^{t,e}$ | Active/ apparent power on power network lines after expansion |
| $U_{t,a}$ | Nodal voltage on power network node $a$, at time $t$ |
| $r_{ne}^e$, $x_{ne}^e$ | New line resistance/ reactance with added cables on line $e$ |
| $TR_j$ | Tightness value of relaxation in SBT |

*Abbreviations*

| | |
|---|---|
| EV | Electric vehicle |
| FC/DWC | Fast charging/dynamic wireless charging |
| FCS | Fast charging station |
| DWCS | Dynamic wireless charging system |
| PV/ESS | Photovoltaic/energy storage system |
| DNO | Distribution network operator |
| PN | Power network |
| TN | Traffic network |
| PTN | Coupled power-traffic network |
| TA | Traffic assignment |
| EDA | Energy demand assignment |
| OBBT | Optimization-based bound tightening |
| SBT | Sequential bound tightening |

## I. Introduction

To ALLEVIATE energy and environmental problems, it has become a global consensus to increase the electric vehicle (EV) penetration [1]. And the rapid increase of EV number will bring a huge charging demand [2]. Under this background, EV charging technologies are paid much attention, and multiple charging methods such as slow charging, fast charging (FC) and dynamic wireless charging (DWC) have been developed to meet the different charging demands of EV users [3]. At the same time, the diversified energy replenishment methods represented by the battery swapping mode is also getting attention [4]. The traffic behavior of EVs affects the traffic flow in the traffic network (TN), and they are also integrated into the power network (PN) through these charging methods [5]. Therefore, providing sufficient charging services while ensuring the efficient operation of the coupled power-traffic network (PTN) has become a key issue [6].

There are several studies that have focused on PTN. Reference [7] provided a steady-state user equilibrium model considering fuel vehicles and EVs in PTN. Reference [8] studied the influence of traffic patterns on the spatial distribution of power loads and proved the advantages of the joint operation of the PTN. Reference [9] considered the possible security threats when the power network and traffic network are coupled. An optimal traffic power flow problem considering power-traffic coupling was proposed in [10]. Reference [11] analyzed the influence of high-permeability electric vehicles on the dependence of power network and traffic network.

Based on the studies of PTN, the optimization of multiple charging methods was studied by several former researches. FC is a widely used charging method that charged EVs through the FC piles. Reference [12] described the distribution of traffic flow in the traffic network by using the unconstrained traffic assignment model. Reference [13] proposed a method of urban electrification planning considering distribution lines, traffic roads and EV charging stations. Reference [14] considered the planning of hybrid energy supply stations which could supply energy for EVs and fuel vehicles at the same time. Reference [15] proposed an EV charging station planning method considering optimal power flow. Reference [16] considered the temporal and spatial characteristics of the traffic network. Reference [17] considered the diversification of objectives based on the urban system, so as to reflect the impact of different factors on the global objective. A planning method that considers the impact of EV charging stations on traffic impacts and power line conditioning capabilities was proposed in [18].

As an innovative charging method, the application of DWC technology has also been widely concerned. Reference [19] studied the DWC demand of city roads and highways. A DWCS planning method aiming at extending EV mileage was proposed in [20]. Reference [21] considered the life cycle of equipment and greenhouse gas emissions in DWCS planning. A DWCS planning method considering traffic wave is proposed in [22]. Although the above studies have covered the application of major charging methods, few researches have studied the complementarity among various charging methods, and the coordinated planning of multiple charging methods. When the charging service provider operates multiple types of charging facilities, having a comprehensive understanding of charging demand information enables the spatial and temporal optimization assignment of charging service capacity and demand [47]. This helps to avoid imbalances in the supply and demand of charging services.

Besides planning and scheduling, the market can also influence both charging service provider and EV users through charging prices. Reference [23] studied the collective charging load scheduling based on real-time charging prices. Reference [24] studied the price elasticity of electric vehicle charging service. Reference [25] considered the dynamic electricity price and the ability of EV charging stations to provide auxiliary services. Reference [26] proposed a dynamic pricing strategy for electric vehicle charging services considering the fluctuation of charging demand and the uncertainty of renewable energy systems. In terms of charging prices, we only need to consider the equilibrium between charging service provider and EV users as two stakeholders but do not necessarily need to know the detailed traffic assignment (TA) result, which complicates the optimization problem and is difficult to solve.

In solving the problem of charging facility planning, some studies regard the charging service provider and the EV user group as a united entity with a shared optimization goal. This approach ignores the game between the charging service provider and the EV user group as two separate stakeholders. In studies taking the game into account, the traffic assignment approach is often adopted to depict the traffic behavior of EV in power-traffic network when charging demand is generated. However, when using the traffic assignment approach, the inner level of the bi-level optimization problem involves a large number of integer variables, leading to high complexity in solving the optimization problem.

To address the above research gaps, we propose a market-based coordinated planning method that considers the game between different stakeholders. In the inner level of the model, we use the energy demand assignment approach instead of the traffic assignment approach, which eliminates integer variables and reduces the complexity of solving the bi-level optimization problem. The main contributions of this paper are listed as follows:

1) The proposed market-based coordinated planning method takes into account the characteristics of DWCSs that do not occupy extra space and allow electric vehicles to be charged during transportation and the low cost of hardware facilities of FCSs. In the coordinated planning model, the complementary characteristics of FCSs and DWCSs in PTN are fully utilized.

2) The EDA approach is adopted to directly assign FC and DWC demand to each road and power node in PTN. All the models required by this method are linear variables, which avoids the influence of integer variables on the solving efficiency.

3) The impact of differentiated traffic demand and differentiated land prices in different regions on planning costs is considered in the case studies. Eight cases based on two PTN in different scale are used to verify the effectiveness of the proposed market-based coordinated planning method.

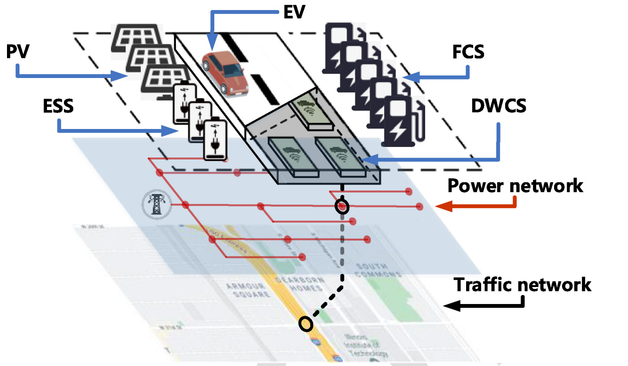


Fig. 1. The Framework of Coupled Power-traffic Network Integrated with FCS and DWCS.

The remainder of the paper is organized as follows: the mathematical models of the market-based coordinated planning method in the coupled network are proposed in Section II. In Section III, the solution of the proposed model is introduced. The case study of the proposed model is validated in Section IV, and Section V concludes.

## II. Mathematical Models of Market-Based Coordinated Planning in PTN

The framework of coupled network integrated with FCSs and DWCSs is illustrated in Fig. 1. In the proposed model, FCSs and DWCSs are responsible for charging the EVs, which provide links between the power network and traffic network. FCSs have the character of cheaper hardware, DWCSs have the characters of taking smaller area and charging on the move. So they have different feasibility for different areas. Their characters enable them to complement each other in the level of planning and operation. PVs can offer electricity to FCSs and DWCSs during the daytime when the rest part of the electricity can be stored in the ESSs. The ESSs charge when the PVs output power is greater than the charging load of FCS and DWCS, and on the contrary if discharges.

### *A. The Interaction Between Charging Service Povider and EV User Group*

The two stakeholders in the model are the charging service providers and EV users. In this paper, we treat all EV users as a collective EV user group [44], [45], [46]. The architecture for the interaction between them is illustrated in Fig. 2. The charging service provider includes the distribution network operator

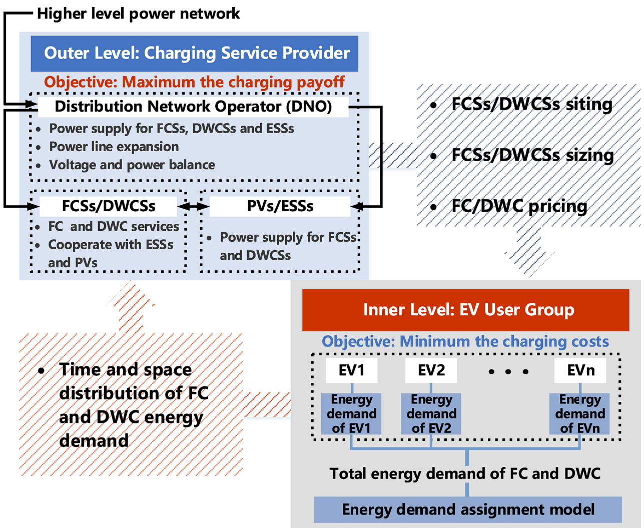


Fig. 2. The interaction between charging service provider and EV user group.

(DNO), FCSs/DWCSs and PVs/ESSs. Within it, the DNO is responsible for providing power supply to FCSs, DWCSs, and ESSs, as well as purchasing electricity from the higher level power network. PVs and ESSs are also responsible for supplying power to FCSs and DWCSs. At the same time, ESSs can accept power supply from the DNO or store energy from PVs that have not been consumed, depending on the scenario and operating conditions. Outer level and inner level represent the benefits of the charging service provider and EV users. Their objectives are maximizing the charging payoff and minimizing the charging costs, respectively. It should be noted that, we mainly focus on the coordinated planning of DWCSs/FCSs, rather than the specific charging navigation strategy of EV individuals. Therefore, as two stakeholders, the charging service provider and the EV user group just share information that does not involve the specific privacy of EV individuals.

The prices of FC/DWC services and the planning schemes of FCSs/DWCSs affect the distribution of energy demand in PTN. In addition, different charging methods will also affect EV users' charging demand. Meanwhile, EV users' charging behavior will affect the sizing and siting of FCSs/DWCSs as well as the charging prices.

Two important concepts should be denoted:

1) Energy gap: the difference between the maximum capacity of EV batteries and the actual energy of EV batteries.

2) Energy demand: the actual demand generated by EVs, that is the energy actually transferred to the electric vehicle through FC and DWC.

### *B. The Energy Demand Assignment Model*

In order to reduce the solving complexity, the EDA model is adopted, as shown in Fig. 2. TA and EDA are compared in the following part to clarify the advantages of EDA.

*1) Traffic Assignment Model (TA):* At the inner-level, the charging scheduling of all the EV users is always regarded as a TA problem. It refers to how to assign traffic demand to roads to minimize transportation costs. In former researches, TA was always solved according to the User Equilibrium or

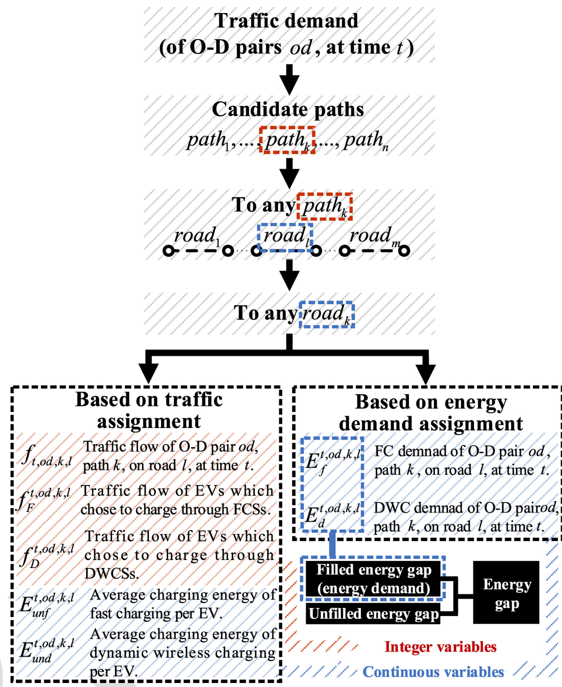


Fig. 3. Comparison of charging schedule based on TA and EDA.

the System Optimization. The TA model based on Nesterov's system is shown as (1)–(4) [13]:

$$\min CH\big(f_{t,od,k,l}\big) \tag{1}$$

$$\text{s.t. } f_{t,od,k,l} \geq 0, \ \ \forall t, od, k, l \tag{2}$$

$$f_F^{t,od,k,l} + f_D^{t,od,k,l} \leq f_{t,od,k,l}, \ \ \forall t, od, k, l \tag{3}$$

$$\sum_{od}\sum_{k} f_{t,od,k,l} \leq V_l, \ \ \forall t, od, k, l \tag{4}$$

where CH is the total charging costs; $f_{t,od,k,l}$ is the traffic flow on time $t$, O-D pair od, path $k$, road $l$; $f_F^{t,od,k,l}$ and $f_D^{t,od,k,l}$ are the traffic flows of EVs which choose to charge through FCSs and DWCSs, respectively. $V_l$ is the maximum vehicle capacity without traffic jams on the road $l$.

As shown in Fig. 3, when simulating the charging scheduling of EVs, integer variables $f_{t,od,k,l}$, $f_F^{t,od,k,l}$, $f_D^{t,od,k,l}$ are necessary for TA. As the number of EVs is an integer, these variables cannot be considered as linear variables. When TA is used in the inner-level of a bi-level problem, the problem will become a bi-level mixed integer programming problem with integer variables in its inner-level, which could be hard to solve [27].

*2) Energy Demand Assignment Model (EDA):* The EDA proposed in this paper is a demand distribution process based on the benefits of charging service provider and EV user group, which directly distributes the charging energy demand to traffic roads and power nodes of PTN. In terms of planning, the specific TA results are not necessary, and we only need to get the EDA results. So the EDA model is proposed to replace the TA model, which is stated as:

$$\min \mathrm{CH}\Big(E_f^{t,od,k,l}, \quad E_d^{t,od,k,l}\Big) \tag{5}$$

$$s.t.\ 0 \leq E_f^{t,od,k,l} + E_d^{t,od,k,l} \leq V_l \eta_{\mathrm{ep}} n_r^l E_u \ \ \forall t, od, k, l \tag{6}$$

$$0 \le \sum_k \sum_l \left( E_f^{t,od,k,l} + E_d^{t,od,k,l} \right) \le E_g^{t,od} \quad \forall t, od, k, l \tag{7}$$

where $E_f^{t,od,k,l}$ and $E_d^{t,od,k,l}$ are the FC/DWC energy demand on time $t$, O-D pair od, path $k$, road $l$; $E_u$ is the average energy gap of each EV; $\eta_{\text{ep}}$ is the EV penetration rate; $n_r^l$ is the number of lanes on the road $l$; $E_g^{t,od}$ is the energy gap on time $t$, O-D pair od. Inequality (6) ensures that the energy demand cannot exceed the maximum energy demand determined by road traffic capacity. Inequality (7) ensures that the energy demand should be less than the upper limit. The proposed EDA requires fewer variables and no integer variables, so that reduces the solving complexity. It should be noted that formulas (5)–(7) are only examples of EDA, and its specific application in the proposed bi-level programming problem will be explained in subsequent chapters.

### C. Outer-Level Objective and Constraints

*1) Outer-Level Objective:* The objective of the outer-level is to maximize the charging payoff, in which the charging service income ($I_{fd}$), the electricity purchasing costs ($C_{pm}$), the penalty costs ($C_{pc}$), the total construction investment ($C_{inv}$) and the operating costs ($C_{op}$) are considered. The outer-level objective is stated as (8):

$$\begin{aligned} \max\ & I_{fd} - C_{op} - C_{pm} - C_{pc} \\ & - C_{inv} \cdot \alpha(1+\alpha)^{\gamma} / \left[(1+\alpha)^{\gamma} - 1\right] \end{aligned} \tag{8}$$

where $\alpha$ is the discount rate; $\gamma$ is the years of investment.

The charging income includes FCS and DWCS charging services income, which is stated as (9). The penalty cost is based on the energy gap that is not met through fast charging or dynamic wireless charging. We believe that as a service-oriented enterprise, charging service provider should also assume basic social responsibilities, some countries and cities have formulated laws and regulations on the service capacity of charging service providers [41], [42]. The penalty costs of the unfilled energy gap are stated as (10).

$$I_{fd} = 365 \sum_t \sum_{od} \sum_k \sum_l \left( E_f^{t,od,k,l} PR_F^t + E_d^{t,od,k,l} PR_D^t \right), \quad \forall t, od, k, l \tag{9}$$

$$C_{pc} = 365 \beta_P \left[ \sum_t \sum_{od} E_g^{t,od} - \sum_t \sum_{od} \sum_k \sum_l \left( E_f^{t,od,k,l} + E_d^{t,od,k,l} \right) \right], \quad \forall t, od, k, l \tag{10}$$

*2) Planning Constraints:* The planning constraints of the proposed model are stated as (11)–(16). The total construction investment includes FCSs, DWCSs, PVs/ESSs installation costs, power network cables expansion costs and the land costs, which is stated as (11). Inequality (12) sets the upper and lower bounds of FCSs and DWCSs. Inequality (13) denotes that the installation capacity of FCSs and DWCSs should be no more than the maximum energy demand. Inequality (14) sets the upper and lower bounds of FC piles, PVs and ESSs. Inequality (15) denotes that the FC piles should only be installed in FCSs. Inequality (16) denotes that PVs and ESSs should only be installed with FCSs and DWCSs.

$$\begin{aligned} C_{inv} = & \sum_e M_{pn}^e PR_{dl} + \sum_l \Big[ (PR_{id} + PR_{dwc} L_l) M_{rd}^l \\ & + PR_{ic} M_{rf}^l + \left( PR_{cp} + PR_{ac}^l \right) n_{cp}^l + \big( PR_{pv} \\ & + PR_{av}^l \big) n_{pv}^l + \left( PR_{es} + PR_{ae}^l \right) n_{es}^l \Big], \ \forall l, e \end{aligned} \tag{11}$$

$$0 \le \sum_l M_{rf}^l \le \mu_F, \ 0 \le \sum_l M_{rd}^l \le \mu_D, \ \forall l \tag{12}$$

$$n_{cp}^l P_F T_u + P_D T_D^{t,l} V_l M_{rd}^l \le V_l \eta_{\text{ep}} n_r^l E_u, \ \forall t, od, k, l \tag{13}$$

$$0 \le n_{cp}^l \le \mu_P, \ 0 \le n_{pv}^l \le \mu_V, \ 0 \le n_{es}^l \le \mu_E, \forall l \tag{14}$$

$$M_{rf}^l \le n_{cp}^l \le \delta_M M_{rf}^l, \forall l \tag{15}$$

$$0 \le n_{es}^l \le \delta_M \left( M_{rf}^l + M_{rd}^l \right), \ 0 \le n_{pv}^l \le \delta_M \left( M_{rf}^l + M_{rd}^l \right), \forall l \tag{16}$$

*3) Operation Constraints:* The operation constraints are stated as (17)–(18). The operating costs include the FCSs operating costs and DWCSs operating costs, which is stated as (17). Equation (18) denotes the electricity purchasing costs:

$$C_{op} = 365 \left( PR_{opf} \sum_l n_{cp}^l + PR_{opd} \sum_l M_{rd}^l L_l \right) T_u, \ \forall l \tag{17}$$

$$C_{pm} = 365 \sum_t \sum_l PR_{pm}^t \left( P_{dn}^{t,l} - P_{pv}^{t,l} \right) T_u, \ \forall t, l \tag{18}$$

*4) ESS State Constraints:* The ESS state constraints are stated as (19)–(24). Inequality (19) denotes that the ESSs cannot be overcharged or over-discharged. Inequality (20) and (21) set the upper and lower bounds of ESSs charging and discharging power. Inequality (22) and (23) ensure that one of $P_{ie}^{t,l}$ and $P_{oe}^{t,l}$ should be 0, which means ESSs are not allowed to charge and discharge at the same time. Equation (24) denotes the ESSs output power to the distributed network. We set the upper and lower limits for the SOC of ESS. Because over-charge and over-discharge of ESS will affect its service life, in this paper, the upper and lower limits of SOC of ESS are set to 0.2 and 0.8 respectively.

$$0.2 n_{es}^l EC_{es} \le EO_l + \sum_{t=1}^{tn} \left( P_{ie}^{t,l} \eta_{ie} + P_{oe}^{t,l} \right) T_u \le 0.8 n_{es}^l EC_{es}, \quad \forall \text{tn} \in [1, 24], \ \forall\ l \tag{19}$$

$$0 \le P_{ie}^{t,l} \eta_{ie} T_u \le 0.8 n_{es}^l EC_{es}, \ \forall t, l \tag{20}$$

$$-0.8 n_{es}^l EC_{es} \le P_{oe}^{t,l} T_u \le 0, \ \forall t, l \tag{21}$$

$$0 \le P_{ie}^{t,l} T_u \le \varepsilon_e^{t,l} \delta_M, \ \forall t, l \tag{22}$$

$$\left( \varepsilon_e^{t,l} - 1 \right) \delta_M \le P_{oe}^{t,l} T_u \le 0, \ \forall t, l \tag{23}$$

$$P_{es}^{t,l} = -\left( P_{ie}^{t,l} + P_{oe}^{t,l} \eta_{oe} \right), \ \forall t, l \tag{24}$$

where $P_{ie}^{t,l}$ and $P_{oe}^{t,l}$ are the input power and output power of the ESSs on the road $l$, at the time $t$; $\eta_{ie}$ and $\eta_{oe}$ are the input and output efficiency of ESSs; $\varepsilon_e^{t,l}$ is the binary variable to guarantee that one of $P_{ie}^{t,l}$ and $P_{oe}^{t,l}$ should be 0; $\delta_M$ is the big constant in the big-M approach; $P_{es}^{t,l}$ is the ESSs output power to the distributed network on the road $l$, at the time $t$.

*5) FC/DWC Prices Constraints:* The FC/DWC price constraints are stated as (25), which are the FC prices and DWC prices constraints, respectively.

$$PR_{pm}^{t} \le PR_{F}^{t} \le PR_{MF},\ \ PR_{pm}^{t} \le PR_{D}^{t} \le PR_{MD},\ \ \forall t \quad (25)$$

*6) Power Network Constraints:* The power network constraints are stated as (26)–(35). Inequality(26) is the constraint on active power output from the power network to FCS and DWCS. Inequality (27) is the constraint on PVs' output power. Equation (28) and inequality (29) are the balance constraints, in which $w$ refers to all power network lines connected to the power network node corresponding to road $l$. Equation of power network line voltage drop is given as (30), in which $a$ and $b$ are power network nodes connected with power network lines $w$. Inequality (31) is the nodal voltage constraint, in which $e$ represents any power network nodes. Equations (32)–(35) are the constraints on the power line resistance and reactance after the power line capacity expansion.

$$0 \le P_{dn}^{t,l} \le \left(M_{rf}^{l} + M_{rd}^{l}\right)\delta_M,\ \forall t, l \quad (26)$$

$$0 \le P_{pv}^{t,l} \le n_{pv}^{l} P_{v}^{t} \ \ ,\forall t, l \quad (27)$$

$$\sum_{w} P_{ad}^{t,w} = P_{bl}^{t,l} + P_{dn}^{t,l} \ \ ,\forall t, l, w \quad (28)$$

$$0 \le S_{ad}^{t,w} \le EC_{or}^{w} + M_{pn}^{w} EC_{pn}, \quad \forall t, w \quad (29)$$

$$U_{t,a} - U_{t,b} = \left(P_{ad}^{t,w} r_{ne}^{w} + Q_{bl}^{t,w} x_{ne}^{w}\right)/U_N, \quad \forall t, w, a, b \quad (30)$$

$$U_m \le U_{t,e} \le U_M,\ \forall t, e \quad (31)$$

$$r_{ne}^{w} = r_{or}^{w} + M_{pn}^{w}\left(r_{com}^{w} - r_{or}^{w}\right),\ \forall w \quad (32)$$

$$x_{ne}^{w} = x_{or}^{w} + M_{pn}^{w}\left(x_{com}^{w} - x_{or}^{w}\right),\ \forall w \quad (33)$$

$$r_{co}^{w} = \left[\left(r_{or}^{w}\right)^2 r_{ad}^{w} + \left(r_{ad}^{w}\right)^2 r_{or}^{w} + \left(x_{or}^{w}\right)^2 r_{ad}^{w} + \left(x_{ad}^{w}\right)^2 r_{or}^{w}\right] / \left[\left(r_{or}^{w} + r_{ad}^{w}\right)^2 + \left(x_{or}^{w} + x_{ad}^{w}\right)^2\right],\ \forall w \quad (34)$$

$$x_{co}^{w} = \left[\left(r_{ad}^{w}\right)^2 x_{or}^{w} + \left(r_{or}^{w}\right)^2 x_{ad}^{w} + \left(x_{or}^{w}\right)^2 x_{ad}^{w} + \left(x_{ad}^{w}\right)^2 x_{or}^{w}\right] / \left[\left(r_{or}^{w} + r_{ad}^{w}\right)^2 + \left(x_{or}^{w} + x_{ad}^{w}\right)^2\right],\ \forall w \quad (35)$$

## D. Inner-Level Objective and Constraints

*1) Inner-Level Objective:* The objective of the inner-level is to minimize the charging costs of EV users, in which the charging service costs ($I_{fd}$) and the charging time costs ($C_{tc}$) are considered. The inner-level objective is stated as:

$$\min \quad I_{fd} + C_{tc} \quad (36)$$

Because the adoption of FC requires additional time for EV users, it incurs the time cost. In existing researches, the method often used is to quantify the time cost by converting it into economic value [48], [49]. In this paper, the wage cost method is used to convert the charging time of EV users into charging time cost. The wage cost method links the time cost of a person with the value that person can create. The charging time costs are stated as (37).

$$C_{tc} = 365 \sum_{t}\sum_{od}\sum_{k}\sum_{l} E_{f}^{t,od,k,l} PR_{hw}/P_F,\ \forall t, od, k, l \quad (37)$$

*2) Energy Demand Constraints:* The energy demand constraints are stated as (38)–(44). Inequality (38) denotes that the energy demand should not exceed the maximum energy demand of O-D pair od, at time $t$. Inequalities (39) and (40) denote that energy demand should not exceed the installation limits of charging facilities. At the same time, constraints (13), (39) and (40) can relax constraint (6) in EDA because they are stricter constraints. Inequality (41) is the constraint on the proportion of EVs with DWC technology. Inequality (42) set the lower bound of total energy demand. Inequalities (43)–(44) ensure that the energy demand should just be assigned on the roads where EVs are passing:

$$0 \le \sum_{k}\sum_{l}\left(E_{f}^{t,od,k,l} + E_{d}^{t,od,k,l}\right) \le E_{g}^{t,od},\ \ \forall t, od, k, l \quad (38)$$

$$0 \le \sum_{od}\sum_{k} E_{f}^{t,od,k,l} \le n_{cp}^{l} P_F T_u,\ \ \forall t, od, k, l \quad (39)$$

$$0 \le \sum_{od}\sum_{k} E_{d}^{t,od,k,l} \le P_D T_D^{t,l} V_l M_{rd}^{l},\ \ \forall t, od, k, l \quad (40)$$

$$0 \le \sum_{k}\sum_{l} E_{d}^{t,od,k,l} \le E_{g}^{t,od}\eta_d,\ \ \forall t, od, k, l \quad (41)$$

$$\lambda_E \sum_{t}\sum_{od} E_{g}^{t,od} \ \le \sum_{t}\sum_{od}\sum_{k}\sum_{l}\left(E_{f}^{t,od,k,l} + E_{d}^{t,od,k,l}\right),\quad \forall t, od, k, l \quad (42)$$

$$0 \le E_{f}^{t,od,k,l} \le M_{ps}^{t,od,k,l}\delta_M,\ \ \forall t, od, k, l \quad (43)$$

$$0 \le E_{d}^{t,od,k,l} \le M_{ps}^{t,od,k,l}\delta_M,\ \ \forall t, od, k, l \quad (44)$$

*3) Coupling Constraints:* Equations (45)–(46) are the coupling constraints on the active/reactive/apparent power which are decided by the power network/PV/ESS output power and the FC/DWC charging power:

$$P_{dn}^{t,l} + P_{pv}^{t,l} + P_{es}^{t,l} = \sum_{od}\sum_{k}\left(E_{f}^{t,od,k,l}/\eta_F \ + E_{d}^{t,od,k,l}/\eta_D\right)\Big/ T_u \quad \forall t, od, k, l \quad (45)$$

$$\sum_{w} S_{ad}^{t,w} = S_{bl}^{t,l} - S_{pv}^{t,l} - S_{es}^{t,l} + \sum_{od}\sum_{k}\left(E_{f}^{t,od,k,l}/\eta_F + E_{d}^{t,od,k,l}/\eta_D\right)\Big/ T_u, \forall t, od, k, l, w \quad (46)$$

# III. Solution of the Proposed Model

## A. Bi-Level Programming Reformulation

To transform the bi-level programming problem into a single-level problem, the KKT conditions are adopted to reformulate the inner-level of the proposed optimization model. The reformulated model contains primal feasible conditions, dual feasible conditions and complementary slackness conditions. The primal feasible conditions are proposed in Section II-D, which include the energy demand constraints (38)–(44) and the coupling constraints (45)–(46). Taking FC as the example, the dual feasible condition is stated as (47). The complementary slackness conditions are stated as (48)–(55).

$$365\left(PR_{F}^{t} + PR_{hw}/P_F\right) - \tau_{f,1}^{t,od} + \tau_{f,2}^{t,od} - \tau_{f,3}^{t,l} + \tau_{f,4}^{t,l} - \tau_{f,5}^{t,od,k,l} - \tau_{f,6} + \tau_{f,7}^{t,od,k,l} + \left(\nu_{f,1}^{t,l} + \nu_{f,2}^{t,l}\right)/(\eta_F T_u) = 0, \quad \forall t, od, k, l \quad (47)$$

$$0 \leq \left[\sum_{k}\sum_{l}\left(E_f^{t,od,k,l}+E_d^{t,od,k,l}\right)\right]\perp\tau_{f,1}^{t,od}\geq 0,\ \forall t,od,k,l \tag{48}$$

$$0 \leq \left[E_g^{t,od}-\sum_{k}\sum_{l}\left(E_f^{t,od,k,l}+E_d^{t,od,k,l}\right)\right]\perp\tau_{f,2}^{t,od}\geq 0,\quad \forall t,od,k,l \tag{49}$$

$$0 \leq \left(\sum_{od}\sum_{k}E_f^{t,od,k,l}\right)\perp\tau_{f,3}^{t,l}\geq 0,\ \forall t,od,k,l \tag{50}$$

$$0 \leq \left(n_{cp}^{l}P_F T_u-\sum_{od}\sum_{k}E_f^{t,od,k,l}\right)\perp\tau_{f,4}^{t,l}\geq 0,\ \forall t,od,k,l \tag{51}$$

$$0 \leq E_f^{t,od,k,l}\perp\tau_{f,5}^{t,od,k,l}\geq 0,\ \forall t,od,k,l \tag{52}$$

$$0 \leq 365\beta_P\left[\sum_{t}\sum_{od}E_g^{t,od}-\sum_{t}\sum_{od}\sum_{k}\sum_{l}\Big(E_f^{t,od,k,l}+E_d^{t,od,k,l}\Big)\right]\perp\tau_{f,6},\ \forall t,od,k,l \tag{53}$$

$$0 \leq \left(E_f^{t,od,k,l}-M_{ps}^{t,od,k,l}\delta_M\right)\perp\tau_{f,7}^{t,od,k,l}\geq 0,\ \forall t,od,k,l \tag{54}$$

where $\tau_{f,1}^{t,od}$-$\tau_{f,7}^{t,od}$ are the dual variables of EDA constraints; $\nu_{f,1}^{t,l}$, $\nu_{f,2}^{t,l}$, $\nu_{d,1}^{t,l}$, $\nu_{d,2}^{t,l}$ are the dual variables of power balance constraints.

## B. Linearization of Complementary Slackness Conditions

The big-M approach is adopted to linearize the bi-linear terms in the complementary slackness conditions. Taking constraint (48) as an example, the linearized constraints of it are stated as (55)–(56).

$$0 \leq \sum_{k}\sum_{l}\left(E_f^{t,od,k,l}+E_d^{t,od,k,l}\right)\leq \varepsilon_{f,1}^{t,od}\delta_M,\ \forall t,od,k,l \tag{55}$$

$$0 \leq \tau_{f,1}^{t,od}\leq\left(1-\varepsilon_{f,1}^{t,od}\right)\delta_M \qquad \forall t,od,k,l \tag{56}$$

where $\varepsilon_{f,1}^{t,od}$ is the auxiliary variable for linearization of complementary slackness conditions.

## C. Linearization of Outer-Level Objective

In the proposed model, $E_f^{t,od,k,l}$, $E_d^{t,od,k,l}$, $PR_F^t$ , $PR_D^t$ are variables so there exist bi-linear terms $E_f^{t,od,k,l}PR_F^t$ and $E_d^{t,od,k,l}PR_D^t$ in the reformulated single-level problem. We adopted the McCormick relaxation approach to linearize these bi-linear terms. We introduce auxiliary variables $BI_f^{t,od,k,l}$ and $BI_d^{t,od,k,l}$ to replace the bi-linear terms $E_f^{t,od,k,l}PR_F^t$ and $E_d^{t,od,k,l}PR_D^t$ respectively, which are stated as (57)–(58). Meanwhile, constraint (9) is reformulated as (59). Taking auxiliary variable $BI_f^{t,od,k,l}$ as the example, the additional constraints on the McCormick relaxation approach are stated as (60)–(63).

$$BI_f^{t,od,k,l}=E_f^{t,od,k,l}PR_F^t,\ \forall t,od,k,l \tag{57}$$

$$BI_d^{t,od,k,l}=E_d^{t,od,k,l}PR_D^t,\qquad \forall t,od,k,l \tag{58}$$

$$I_{fd}=365\sum_{t}\sum_{od}\sum_{k}\sum_{l}\left(BI_f^{t,od,k,l}+BI_d^{t,od,k,l}\right),\quad \forall t,od,k,l \tag{59}$$

$$BI_f^{t,od,k,l}\geq PR_{pm}^{t}E_f^{t,od,k,l},\quad \forall t,od,k,l \tag{60}$$

$$BI_f^{t,od,k,l}\geq \mu_P P_F T_u PR_F^t+PR_{MF}E_f^{t,od,k,l}-\mu_P P_F T_u PR_{pm}^t,\ \forall t,od,k,l \tag{61}$$

$$BI_f^{t,od,k,l}\leq PR_{MF}E_f^{t,od,k,l},\qquad \forall t,od,k,l \tag{62}$$

$$BI_f^{t,od,k,l}\leq \mu_P P_F T_u PR_F^t+PR_{pm}^{t}E_f^{t,od,k,l}-\mu_P P_F T_u PR_{pm}^t,\ \forall t,od,k,l \tag{63}$$

## D. Linearization of Nodal Voltage Constraints

When combining (30) with (32) and (33), (30) will be reformulated as (64), which contains nonlinear term $P_{ad}^{t,e}M_{pn}^{e}$. We introduce auxiliary variables $UP_{t,e}$ to replace the term $P_{ad}^{t,e}M_{pn}^{e}$. Then we adopted the big-M approach to linearize constraint (64) and reformulate it as (65)–(67).

$$U_{t,a}-U_{t,b}=\Big[P_{ad}^{t,e}r_{or}^{e}+Q_{bl}^{t,e}x_{or}^{e}+\left(r_{co}^{e}-r_{or}^{e}\right)P_{ad}^{t,e}M_{pn}^{e}+\left(x_{co}^{e}-x_{or}^{e}\right)Q_{bl}^{t,e}M_{pn}^{e}\Big]/U_N,\ \forall t,e,a,b \tag{64}$$

$$U_{t,a}-U_{t,b}=\Big[P_{ad}^{t,e}r_{or}^{e}+Q_{bl}^{t,e}x_{or}^{e}+\left(r_{co}^{e}-r_{or}^{e}\right)UP_{t,e}+\left(x_{co}^{e}-x_{or}^{e}\right)Q_{bl}^{t,e}M_{pn}^{e}\Big]/U_N,\ \forall t,e,a,b \tag{65}$$

$$0\leq UP_{t,e}\leq P_{ad}^{t,e},\qquad \forall t,e \tag{66}$$

$$P_{ad}^{t,e}-\left(1-M_{pn}^{e}\right)\delta_M\leq UP_{t,e}\leq M_{pn}^{e}\delta_M,\ \forall t,e \tag{67}$$

## E. Linearization of Nodal Voltage Constraints

The McCormick relaxation can lead to inaccurate approximate solutions during model solving. In order to provide tighter valid bounds to the relaxed optimal problem solving step, an OBBT-SBT-based approach that combines optimization-based bound tightening (OBBT) with sequential bound tightening (SBT) is employed [32]. Firstly, the OBBT method is employed to derive the valid bounds of variables. Based on the results of OBBT, the SBT method is employed to further tighten the relaxation.

*1) OBBT Method:* We first employ the OBBT method to improve the bounds of the relaxed optimal problem. Defining $B_u^i$ and $B_l^i$ as the upper/lower bound set of variables at the $i$th iteration. There are two models for the upper/lower bound of the OBBT method, and the objectives of which are stated as (68) and (69), respectively. $\varepsilon$ in the added constraint (70) represents a local feasible solution of the original bi-level problem:

$$F_u:\ \min\ B_u \tag{68}$$

$$F_l:\ \min\ B_l \tag{69}$$

$$\text{s.t. } I_{fd}-C_{op}-C_{inv}\cdot\left[(1+\alpha)^{\gamma}-1\right]/\alpha\gamma^{2}\geq\varepsilon \tag{70}$$

(9)–(67)

The solving process of the OBBT method is presented in Algorithm 1. In line 1, the tolerance values of upper/lower bound ($tv_u$, $tv_l$), original upper/lower bounds ($B_u^0$, $B_l^0$) are input. The ending condition of the iteration in lines 3–7 is that the $l^{\infty}$ norms between two adjacent iteration results less than the tolerance values. In line 4, the $i$th iteration results are drawn through $F_u$ and $F_l$. In line 5, the upper and lower bounds of $i-1$th iteration and $i$th iteration are compared and

**Algorithm 1** OBBT Method

1: **input:** $tv_u$, $tv_l$, $B_u^0$, $B_l^0$
2: **initialize:** $i = 1$
3: **while** $(\|B_u^i - B_u^{i-1}\|_\infty < tv_u) \&\& (\|B_l^i - B_l^{i-1}\|_\infty < tv_l)$
4: $[B_u^i] = F_u(B_u^{i-1})$, $[B_l^i] = F_l(B_l^{i-1})$
5: $B_u^i = \min(B_u^i, B_u^{i-1})$, $B_l^i = \max(B_l^i, B_l^{i-1})$
6: $i = i + 1$
7: **end**

**Algorithm 2** SBT Method

1: **input:** $tv_s$, $\{\psi^j\}_{j=1}^J$, $B_{su}^0$, $B_{sl}^0$
2: **initialize:** $j = 1$
3: **while** $TR_j \leq tv_s$
4: $[B_{cu}^j] = F_o(B_{su}^{j-1},\ B_{sl}^{j-1})$
5: $B_{su}^j = (1 + \psi^j)B_{cu}^j$, $B_{sl}^j = (1 - \psi^j)B_{cu}^j$
6: $j = j + 1$
7: **end**

the tighter bounds are assigned to $B_u^i$ and $B_l^i$. The proofs of parallelizability and convergence are shown in [33].

*2) SBT Method:* Based on the results of the OBBT method, we adopted the SBT method to further improve the tightness of bounds [32], which is presented in Algorithm 2.

Defining $B_{su}^j$ and $B_{sl}^j$ as the upper/lower bound sets of variables at the $j$th iteration. The original upper/lower bounds after tightening with OBBT method ($B_{su}^0$, $B_{sl}^0$), the convergence tolerance ($tv_s$) and a decreasing sequence ($\{\psi^j\}_{j=1}^J$) are input in line 1. Lines 3–7 represent the iteration function, and the ending condition is that the tightness value of relaxation ($TR_j$) is not greater than the convergence tolerance $tv_s$. The $TR_j$ is measured as the absolute value of the difference between the actual variables and the auxiliary variables, which is denoted in (71). The $F_o$ represents the optimal problem after dealing with the linearizing processes in chapters 3.1-3.4. The current bound of the $j$th iteration ($B_{cu}^j$) is worked out based on the upper and lower bounds of $j-1$th iteration ($B_{su}^{j-1}$, $B_{sl}^{j-1}$). Finally, the upper and lower bounds of $j$th iteration ($B_{su}^j$, $B_{sl}^j$) are updated based on the $B_{cu}^j$.

$$\mathrm{TR} = \Big|\sum\sum\sum\sum\Big(BI_{df}^{t,od,k,l} + BI_{df}^{t,od,k,l} - E_{df}^{t,od,k,l}PR_F^t - E_{dd}^{t,od,k,l}PR_D^t\Big)\Big/\Big(E_{df}^{t,od,k,l}PR_F^t + E_{dd}^{t,od,k,l}PR_D^t\Big)\Big|, \quad \forall t, od, k, l \tag{71}$$

## IV. Case Study

In this section, we apply the proposed market-based coordinated planning method to the 21 power nodes-12 traffic nodes network (P21-T12 network) and the 54 power nodes-25 traffic nodes network (P54-T25 network). The parameter settings are listed in Table I [28], [29], [30], [31]. The time-of-use (TOU) electricity price is adopted to simulate the fluctuation of electricity price [39], [40]. The baseload curve and the traffic demand curve are represented as per-unit values, which are shown in Fig. 4 [22]. The reference values of which are the installation capacities of each power node. In order to reflect the influence of environmental factors on PVs output power, eight typical scenarios of PVs output power [37] are proposed in this paper according to the difference of seasons (spring, summer, autumn and winter) and light intensity (high radiation, low radiation), as shown in Fig. 5(a) and Fig. 5(b). Fig. 5(a) is the PV daily output power curve of high radiation days, while Fig. 5(b) is the PVs daily output power curve of low radiation days. According to historical data [38], the number of high radiation days in spring, summer, autumn and winter was selected as 22, 25, 19 and 13 respectively. The simulation cases are operated based on the MATLAB 2019a platform in CPLEX with Intel Core i7-9750H, 32 GB of memory.

TABLE I
PARAMETER SETTINGS

| Param. | Val. | Param. | Val. | Param. | Val. |
|---|---|---|---|---|---|
| $\alpha$ | 0.05 | $\mu_V$ | 4MW | $PR_{dwc}$ | $1\times10^5$ \$ |
| $\gamma$ | 20 | $\mu_E$ | 4MWh | $PR_{pv}$ | $7.8\times10^4$ \$/MW |
| $E_u$ | 22.5kWh | $\eta_{DWC}$ | 0.8 | $PR_{es}$ | $1.2\times10^5$ \$/MWh |
| $T_u$ | 1h | $\eta_{ep}$ | 0.8 | $PR_{opf}$ | 1.5\$/h |
| $P_F$ / $P_D$ | 44/40 kW | $U_N$ | 10kV | $PR_{opd}$ | 83\$/h |
| $\eta_{ie}$ / $\eta_{oe}$ | 0.9/0.9 | $U_m$ / $U_M$ | 9.5/10.5 kV | $PR_{dl}$ | $3\times10^5$ \$ |
| $\eta_F$ / $\eta_D$ | 0.92/ 0.9 | $PR_{ic}$ | $1.63\times10^5$ \$ | $PR_{hw}$ | 20\$/h |
| $\lambda_E$ | 0.6 | $PR_{id}$ | $5\times10^4$ \$ | $\beta_P$ | 0.1\$/kWh |
| $\mu_P$ | 400 | $PR_{cp}$ | $4\times10^3$ \$ | $EC_{es}$ | 100 kWh |

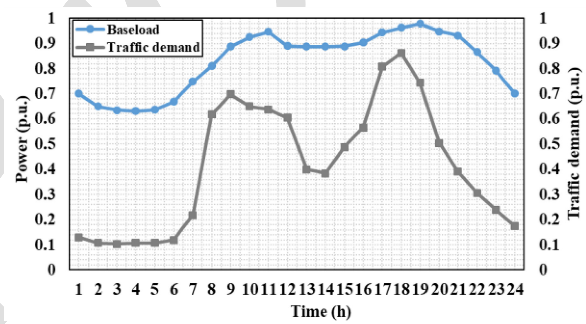


Fig. 4. Baseload curve and traffic demand curve.

### A. Case Studies Based on P21-T12 Network

The 21 power nodes-12 traffic nodes network (P21-T12 network) is adopted in this Section [14]. It consists of twenty-one power nodes, twelve traffic nodes and twelve traffic roads. There are eight connection nodes between power network and traffic network, which make the network coupled. In this network, road T4-T8 belongs to the urban area when other roads belong to suburban areas. In this paper, there is no restriction on the construction area of FCSs and DWCSs. They are allowed to be constructed in urban or suburban areas. The topology of it is shown in Fig. 6. In this section, we adopt

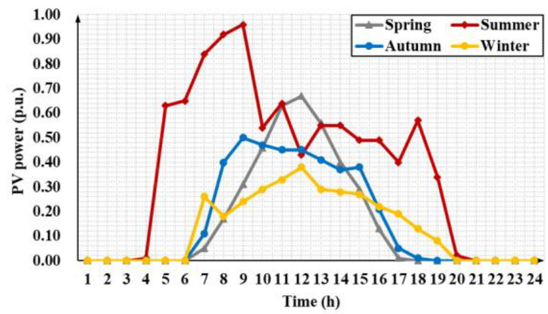


(a) High radiation days.

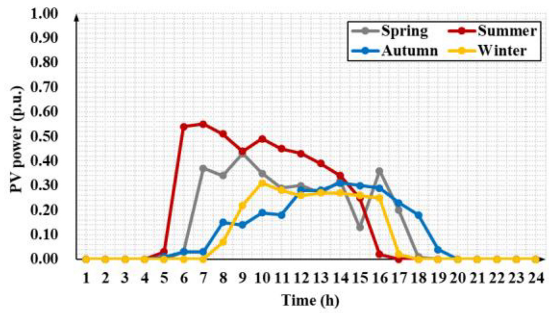


(b) Low radiation days.

Fig. 5. PV daily output power curves of different seasons.

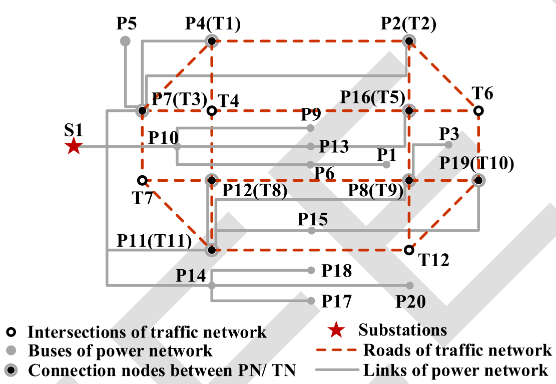


Fig. 6. Topology of P21-T12 network.

three cases based on the P21-T12 network, which are shown as follows: in Case 1, install both FCSs and DWCSs in the P21-T12 network and set both the maximum numbers of FCSs and DWCSs as five; in Case 2, only install FCSs in the P21-T12 network and set the maximum number of FCSs as five; in Case 3, only install DWCSs in the P21-T12 network and set the maximum number of DWCSs as five. The number of EV trips in these cases is $5 \times 10^4$. The size of the EV batteries is 75kWh.

According to the proposed planning method, the sites of FCSs, DWCSs and additional power cables of Case 1 are shown in Fig. 7(a). As the comparison cases, Case 2 and Case 3 are also simulated based on the P21-T12 network. The sites of FCSs, DWCSs and additional power cables of Case 2 and Case 3 are shown in Fig. 7(b) and Fig. 7(c), respectively.

The detailed planning results of the above cases are listed in Table II. In Table II, Px-Ty1-Ty2(a, b, c) and Px-Ty1-Ty2(b, c) represent the FCS and DWCS planning results, respectively. Px is the corresponding power network node of the road

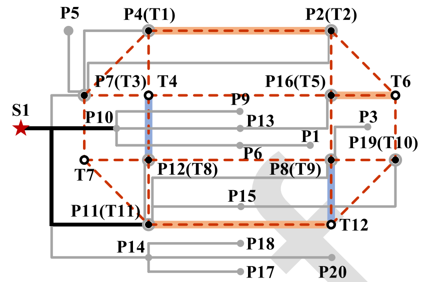

(a) Case 1: Install both FCSs and DWCSs.

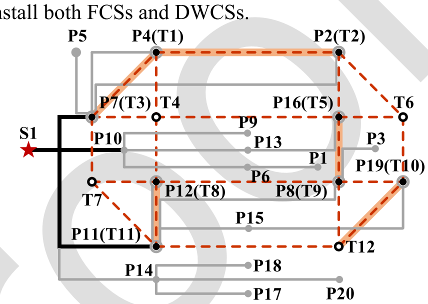

(b) Case 2: Only install FCSs.

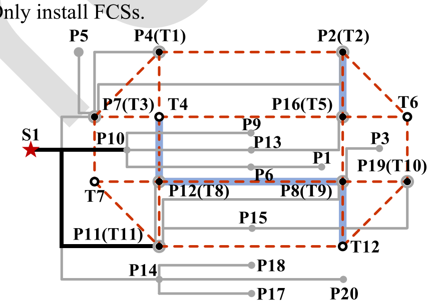

(c) Case 3: Only install DWCSs.

Roads installed with both FCSs /DWCSs — Links installed with added cables
Roads installed with DWCSs — Roads installed with FCSs

Fig. 7. FCSs/DWCSs siting and power cables expansion results of Case 1-3.

TABLE II
DETAILED PLANNING RESULTS BASED ON P21-T12 NETWORK

| | | Planning results |
|---|---|---|
| Case 1 | FCSs | P4-T1-T2(140,4,4); P16-T5-T6(140,4,4); P11-T11-T12(130,3,3) |
| | DWCSs | P12-T8-T4(0,0); P19-T10-T12(0,0) |
| | Power lines | S1-P10; S1-P11 |
| Case 2 | FCSs | P7-T3-T1(240,6,6); P4-T1-T2(200,5,5); P16-T5-T9(200,5,5); P11-T11-T8(240,6,6); P19-T10-T12(120,3,3) |
| | Power lines | S1-P7; S1-P10; S1-P11 |
| Case 3 | DWCSs | P16-T5-T2(0,0); P12-T8-T4(0,0); P8-T9-T12(0,0); P12-T8-T9(0,0) |
| | Power lines | S1-P10; S1-P11 |

planned with FCS (DWCS); Ty1 and Ty2 are the side nodes of roads; a, b, c are the numbers of charging piles, PV (unit capacity: 100 kW), and ESS (unit capacity: 100 kWh).

In Fig. 7(a), the only two DWCSs are installed on T4-T8 and T9-T12. In Fig. 7(c), T4-T8 is also installed with DWCS. It is because that urban roads are more suitable for DWCS: the traffic flow of urban roads is larger, which can provide larger DWC energy demands. Meanwhile, DWCS has the character of saving land costs, the high land price in urban areas has little impact on its investment cost.

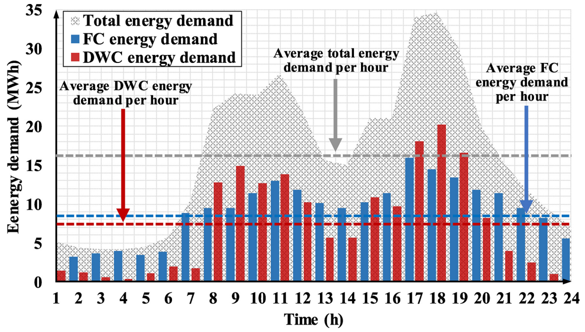


Fig. 8. Energy demand of Case 1.

TABLE III
ECONOMIC RESULTS BASED ON P21-T12 NETWORK

| | Case 1 | Case 2 | Case 3 |
|---|---|---|---|
| $C_{inv}$ /\$ (annual) | $1.79\times10^6$ | $2.15\times10^6$ | $2.32\times10^5$ |
| $C_{pm}$ /\$ | $2.74\times10^6$ | $2.39\times10^6$ | $2.78\times10^6$ |
| $C_{op}$ /\$ | $9.59\times10^6$ | $5.45\times10^6$ | $1.07\times10^7$ |
| $I_{fd}$ /\$ | $2.15\times10^7$ | $1.87\times10^7$ | $2.05\times10^7$ |
| $C_{tc}$ /\$ | $1.73\times10^7$ | $3.16\times10^7$ | 0 |
| $C_{pc}$ /\$ | $2.83\times10^6$ | $5.60\times10^6$ | $4.25\times10^6$ |
| Charging payoff /\$ | $4.54\times10^6$ | $3.11\times10^6$ | $4.54\times10^5$ |
| Users' charging costs /\$ | $3.88\times10^7$ | $5.03\times10^7$ | $2.05\times10^7$ |

Fig. 8 shows the energy demand of Case 1. In Fig. 8, the energy demand of DWC fluctuates more violently with traffic demand than that of FCS, which means DWC energy demand is influenced more by traffic demand. The average hourly energy demand is 16.17 MWh. Within it, the energy demand proportion of FC and DWC are 55.91% and 44.09%, indicating that EV owners generally have the same dependence on FC and DWC in this scenario. During the peak periods (8 a.m. to 12 a.m. and 4 p.m. to 8 p.m.), the energy demand of DWC is higher than that of FC. During the off-peak periods, the energy demand of FC is significantly higher than that of DWC. In general, the ratio of FC to DWC energy demand decreases with the increase of total charging energy demand. During peak hours, the traffic flow on urban roads is greater and DWCSs are mainly constructed in urban areas, so DWCSs have higher charging energy demand during peak hours, while the case is on the contrary during off-peak hours.

The economic results are shown in Table III. The planning scheme of Case 1 is the most economical one to charging service provider, while that of Case 3 is the friendliest one to EV users. In the aspect of penalty costs, the penalty costs of Case 3 are almost about twice as much as that of Case 1. It means that the advantage of Case 3 in EV users charging costs is based on far lower energy demand which is satisfied.

In the aspect of charging service provider, the charging service provider's charging payoff in Case 2 is dramatically lower than that in Case 1, which means Case 1 can meet more energy demand and is more economical. It is mainly because that installing FCSs in urban areas is avoided for the sack of land costs, the possible high energy demand in urban areas

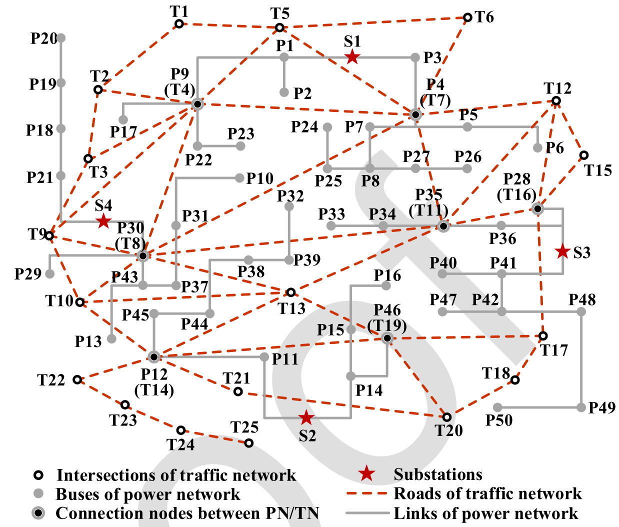


Fig. 9. Topology of P54-T25 network.

is abandoned in Case 2, which can significantly reduce the charging income.

When comparing Case 1 with Case 3, a similar conclusion can be drawn. It is mainly because that the investment costs of DWCSs are more expensive than FCSs in some suburban areas when meeting the same quantity of energy demand. In the aspect of EV users, the charging costs of Case 3 are lowest while that of Case 2 is the highest. It is mainly because that it takes time to charge when using FC but DWCSs do not take extra time of EV users.

According to the analysis above, installing DWCSs in urban areas can capture the high energy demand in these areas and save the massive land costs; installing FCSs in suburban areas can satisfy the energy demand of these areas and cost far fewer investment costs of devices than DWCSs. Coordinated planning has the advantages of meeting more energy demand and being more economical.

### *B. Case Studies Based on P54-T25 Network*

The 54 power nodes-25 traffic nodes network (P54-T25 network) is adopted in this Section [14]. It consists of fifty-four power nodes, twenty-five traffic nodes and twenty traffic roads. There are seven connection nodes between power network and traffic network, which make the network coupled. In this network, roads T5-T6, T6-T7, T7-T11, T7-T12 and T11-T12 belong to the urban areas when other roads belong to suburban areas. The topology of it is shown in Fig. 9.

In this section, we work out three cases based on the P54-T25 network, which are shown as follows: in Case 4, install both FCSs and DWCSs in the P54-T25 network and set both the maximum numbers of FCSs and DWCSs as ten; in Case 5, only install FCSs in the P54-T25 network and set the maximum number of FCSs as twenty; in Case 6, only install DWCSs in the P54-T25 network and set the maximum number of DWCSs as twenty. The number of EV trips in these cases is $1\times10^5$. The size of the EV batteries is 75kWh. It should be noted that this paper focuses on the impact of the proposed planning method on charging service provider

TABLE IV
DETAILED PLANNING RESULTS BASED ON P54-T25 NETWORK

| | | Planning results |
|---|---|---|
| Case 4 | FCSs | P9-T4-T3(170,10,7); P9-T4-T5(140,7,6); P9-T4-T9(90,12,8); P30-T8-T9(100,10,8); P30-T8-T13(160,20,9); P12-T14-T10(160,19,7); P12-T14-T13(120,5,5); P46-T19-T13(160,20,8); P46-T19-T17(160,18,10); P46-T19-T20(160,15,9) |
| | DWCSs | P4-T7-T4(22,10); P4-T7-T5(40,8); P4-T7-T11(26,10); P4-T7-T12(40,9);P30-T8-T10(28,9) |
| | Power lines | S1-P1; S1-P3; P1-P9; P3-P4; S2-P14; P14-P46; S4-P30 |
| Case 5 | FCSs | P3-T7-T4(120,10,15); P4-T7-T8(60,10,5); P9-T4-T2(160,16,8); P9-T4-T4(130,14,10); P9-T4-T5(50,8,6); P9-T4-T8(160,20,24); P9-T4-T9(80,12,17); P12-T14-T10(100,15,3); P12-T14-T13(160,22,5); P12-T14-T21(120,20,7); P12-T14-T22(180,19,4); P30-T8-T9(180,27,10); P30-T8-T10(110,20,7); P30-T8-T13(180,24,10); P30-T8-T11(160,14,16); P35-T11-T13(120,5,5); P46-T19-T13(210,23,9); P46-T19-T14(160,14,8); P46-T19-T17(170,26,14); P46-T19-T20(140,25,9) |
| | Power lines | S1-P1; P1-P9; S1-P3; P3-P4;S2-P11; P11-P12; S2-P14; P14-P46; S4-P30 |
| Case 6 | DWCSs | P4-T7-T6(12,15); P4-T7-T11(22,16); P9-T4-T7(18,12); P9-T4-T8(26,10); P30-T8-T9(10,8); P12-T14-T13(30,6); P12-T14-T19(24,8); P30-T8-T10(26,9); P30-T8-T13(19,7); P35-T11-T16(40,0); P35-T11-T13(20,14); P35-T11-T12(18,12) |
| | Power lines | S1-P1; P1-P9; S1-P3; P3-P4; S2-P11; P11-P12; S3-P36; P36-P35; S4-P30 |

and EV user group, and does not consider the impact of the planning scheme on other social entities.

According to the proposed market-based coordinated planning method, the planning sites of FCSs, DWCSs and additional power cables of Case 4 are shown in Fig. 10(a). As the comparison cases, Case 5 and Case 6 are also simulated based on the P54-T25 network. The planning sites of FCSs, DWCSs and additional power cables of Case 5 and Case 6 are shown in Fig. 10(b) and Fig. 10(c), respectively. The detailed planning results of the cases are listed in Table IV.

The planning sites of FCSs and DWCSs in the P54-T25 network are similar to those in the P21-T12 network. In Fig. 10(a), all the ten FCSs are installed in suburban areas, and three of the five DWCSs are installed in urban areas. In Fig. 10(b), there are twenty FCSs are installed in the network. Even in the condition that the number of FCSs reaches the upper limit, there is still no FCS installed in the urban area due to the high land costs. On the contrary, there are three urban roads installed with DWCSs. It indicates that DWCSs are more economical than FCSs in urban areas. In the aspect of power cables expansion, all three cases expand the power cables very concentrated. It is because that most of the roads installed with FCSs or DWCSs are connected to P4, P7, P12, P19 and P30. The concentration of charging load can help to reduce the number of power cables that need to be expanded, thus reducing investment costs.

Fig. 11 shows the energy demand of Case 4, according to it, the average hourly charging energy demand in a typical day of Case 4 is 30.05MWh; the energy demand of FC and DWC

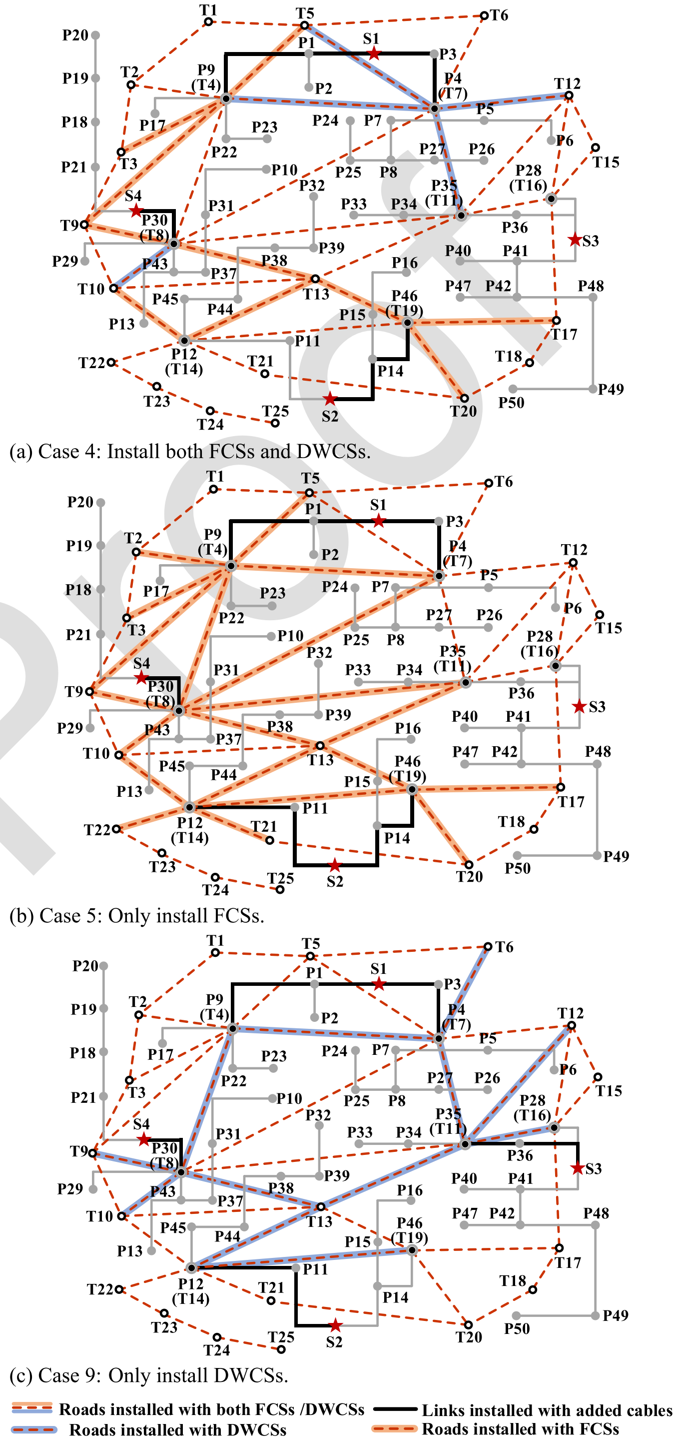


(a) Case 4: Install both FCSs and DWCSs.

(b) Case 5: Only install FCSs.

(c) Case 9: Only install DWCSs.

Fig. 10. FCSs/DWCSs siting and power cables expansion results of Case 4-6.

are 17.75MWh and 12.30MWh, respectively, accounting for 59.06% and 40.94% of the total energy demand. Compared with Case 1, the proportion of FC energy demand in Case 4 is significantly higher. As shown in Fig. 10(a), the number of FCSs is far more than DWCSs. It indicates that EV users have greater reliance on FC in a bigger network.

The economic results are shown in Table V. Case 4-Case 6 simulate the scene that the energy demand is much larger than the charging service resources. In this scene, the

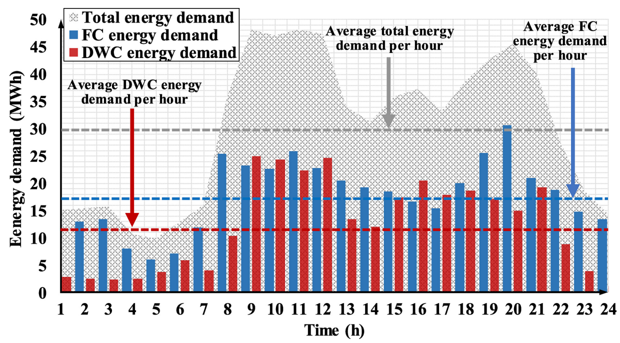


Fig. 11. Energy demand of Case 4.

TABLE V
ECONOMIC RESULTS BASED ON P54-T25 NETWORK

| | Case 4 | Case 5 | Case 6 |
|---|---|---|---|
| $C_{inv}$ /$ (annual) | $7.99\times10^{6}$ | $1.27\times10^{7}$ | $9.02\times10^{6}$ |
| $C_{pm}$ /$ | $8.31\times10^{6}$ | $8.10\times10^{6}$ | $8.54\times10^{6}$ |
| $C_{op}$ /$ | $2.36\times10^{7}$ | $1.27\times10^{7}$ | $3.01\times10^{7}$ |
| $I_{fd}$ /$ | $5.24\times10^{7}$ | $4.46\times10^{7}$ | $5.62\times10^{7}$ |
| $C_{tc}$ /$ | $7.18\times10^{7}$ | $1.11\times10^{8}$ | 0 |
| $C_{pc}$ /$ | $6.10\times10^{6}$ | $6.31\times10^{6}$ | $6.61\times10^{6}$ |
| Charging payoff /$ | $6.40\times10^{6}$ | $4.79\times10^{6}$ | $1.93\times10^{6}$ |
| Users' charging costs /$ | $1.24\times10^{8}$ | $1.57\times10^{8}$ | $5.62\times10^{7}$ |

TABLE VI
COMPUTING TIME OF THE PLANNING METHODS BASED ON EDA AND TA

| | Case 1 | Case 4 | Case 7 | Case 8 |
|---|---|---|---|---|
| Networks | P21-T12 | P54-T25 | P21-T12 | P54-T25 |
| Methods | Based on EDA | Based on EDA | Based on TA | Based on TA |
| Computing time/ s | $1.12\times10^{4}$ | $1.89\times10^{4}$ | $2.01\times10^{4}$ | $3.94\times10^{4}$ |
| Charging payoff /$ | $4.54\times10^{6}$ | $6.40\times10^{6}$ | $4.11\times10^{6}$ | $5.36\times10^{6}$ |
| Users' charging costs /$ | $3.88\times10^{7}$ | $1.24\times10^{8}$ | $4.07\times10^{7}$ | $1.27\times10^{8}$ |

penalty costs of Case 4-Case 6 are close, but the charging payoff of Case 4 is much greater than that of Case 5 and Case 6. It means that in the extreme scenes with a huge energy gap, the proposed method is still economical.

In order to further validate the effectiveness of the proposed planning method, we construct case 7 and case 8 to compare with case 1 and case 4 respectively. Both case 7 and case 8 adopt the TA model [43], and they are constructed based on P21-T12 network and P54-T25 network, respectively.

Table VI compares the computing time, charging payoff and users' charging costs of case 1, case 4, case 7 and case 8. As can be seen from the table, when the same planning method is adopted, a larger network consumes more computing time. When using the same network, the computing time of the planning methods based on TA is longer than that of the planning methods based on EDA, which is due to the large number of integer variables in TA. It will greatly reduce the calculation efficiency of the planning method. In terms of economy, for cases based on the same network, the application of the EDA-based planning method will lead to higher charging payoff for charging service provider and lower users' charging costs.

## V. CONCLUSION

Firstly, a market-based coordinated planning model was proposed, whose outer-level objective is to maximize the charging service profit of the charging service provider and the inner-level objective is to minimize the total charging cost of the EV users. The siting and sizing plans of FCSs/DWCSs/PVs/ESSs, the expansion plan of power network cables and the charging prices of FC and DWC are the main decision variables of the outer-level problem. The spatial-temporal distribution of FC and DWC energy demands are the main decision variables of the inner-level problem. Secondly, the EDA model is proposed to simulate the distribution of charging energy demand in the inner-level problem, which avoids integer variables in the traditional TA model, thus reducing the solving complexity of the bi-level programming problem. Then the bi-level programming problem is reconstructed into a single-level programming problem by KKT condition, and the linearization of the reconstructed problem was performed by the Big-M method and McCormick relaxation method. On this basis, the OBBT-SBT method is used to tighten the variable boundary, so as to obtain a tighter boundary. Finally, in the case study, six scenarios based on the P21-T12 network and the P54-T25 network are used to verify the effectiveness of the market-based coordinated planning method. The simulation results show that FCS and DWCS have significant complementary characteristics in terms of economy in the case of differentiated land prices, and the proposed method can make the most of this feature, improve the charging service profit of charging service provider, and keep the total charging cost of EV users in a relatively low range.

In the future research, the research content of this paper can be used as the basis of the EV charging navigation problem. EV charging navigation can provide specific charging schemes for EV individuals, including the selection of charging stations, charging paths and charging time [35]. Because this paper mainly studies the planning problem, it does not specifically consider the charging behavior of EV individuals. In the future research, we will consider the charging behavior characteristics of EV individuals, such as the uncertainty and bounded rationality of charging time and charging path selection [36].

## REFERENCES

[1] H. Wang, Z. Yan, X. Xu, and K. He, "Probabilistic power flow analysis of microgrid with renewable energy," *Int. J. Elect. Power*, vol. 114, Jan. 2020, Art. no. 105393.

[2] X. Lu, S. Xia, W. Gu, K. Chan, and M. Shahidehpour, "Two-stage robust distribution system operation by coordinating electric vehicle aggregator charging and load curtailments," *Energy*, vol. 226, Jul. 2021, Art. no. 120345.

[3] M. Khodayar, L. Wu, and Z. Li, "Electric vehicle mobility in transmission-constrained hourly power generation scheduling," *IEEE Trans. Smart Grid*, vol. 4, no. 2, pp. 779–788, Jun. 2013.

[4] M. Ban, J. Yu, M. Shahidehpour, D. Guo, and Y. Yao, "Electric vehicle battery swapping-charging system in power generation scheduling for managing ambient air quality and human health conditions," *IEEE Trans. Smart Grid*, vol. 10, no. 6, pp. 6812–6825, Nov. 2019.

[5] Y. Sun, Z. Chen, Z. Li, W. Tian, and M. Shahidehpour, "EV charging schedule in coupled constrained networks of transportation and power system," *IEEE Trans. Smart Grid*, vol. 10, no. 5, pp. 4706–4716, Sep. 2019.

[6] S. Xie, Z. Hu, and J. Wang, "Two-stage robust optimization for expansion planning of active distribution systems coupled with urban transportation networks," *Appl. Energy*, vol. 261, Mar. 2020, Art. no. 114412.

[7] W. Wei, L. Wu, J. Wang, and S. Mei, "Network equilibrium of coupled transportation and power distribution systems," *IEEE Trans. Smart Grid*, vol. 9, no. 6, pp. 6764–6779, Nov. 2018.

[8] W. Wei, S. Mei, L. Wu, M. Shahidehpour, and Y. Fang, "Optimal traffic-power flow in urban electrified transportation networks," *IEEE Trans. Smart Grid*, vol. 8, no. 1, pp. 84–95, Jan. 2017.

[9] Y. Sheng, Q. Guo, T. Yang, Z. Zhou, and H. Sun, "A potential security threat and its solution in coupled urban power-traffic networks with high penetration of electric vehicles," *CSEE J. Power Energy Syst.*, vol. 8, no. 4, pp. 1097–1109, Jul. 2022.

[10] T. Zhao, H. Yan, X. Liu, and Z. Ding, "Congestion-aware dynamic optimal traffic power flow in coupled transportation power systems," *IEEE Trans. Ind. Informat.*, vol. 19, no. 2, pp. 1833–1843, Feb. 2023.

[11] Y. Zhang, S. Xie, and S. Shu, "Decentralized optimization of multi-area interconnected traffic-power systems with wind power uncertainty," *IEEE Trans. Ind. Informat.*, vol. 19, no. 1, pp. 133–143, Jan. 2023.

[12] X. Wang, M. Shahidehpour, C. Jiang, and Z. Li, "Coordinated planning strategy for electric vehicle charging stations and coupled traffic-electric networks," *IEEE Trans. Smart Grid*, vol. 32, no. 1, pp. 268–279, Jan. 2019.

[13] W. Wei, L. Wu, J. Wang, and S. Mei, "Expansion planning of urban electrified transportation networks: A mixed-integer convex programming approach," *IEEE Trans. Transport. Electrific.*, vol. 3, no. 1, pp. 210–224, Mar. 2017.

[14] W. Gan et al., "Two-stage planning of network-constrained hybrid energy supply stations for electric and natural gas vehicles," *IEEE Trans. Smart Grid*, vol. 12, no. 3, pp. 2013–2026, May 2021.

[15] C. Wang, R. Dunn, F. Robinson, B. Lian, W. Yuan, and M. Redfern, "Active–reactive power approaches for optimal placement of charge stations in power systems," *Int. J. Elect. Power Energy Syst.*, vol. 84, pp. 87–98, Jan. 2017.

[16] S. Li, Y. Huang, and S. J. Mason, "A multi-period optimization model for the deployment of public electric vehicle charging stations on network," *Transp. Res. Part C Emerg. Technol.*, vol. 65, pp. 128–143, Apr. 2016.

[17] Q. Cui, Y. Weng, and C.-W. Tan, "Electric vehicle charging station placement method for urban areas," *IEEE Trans. Smart Grid*, vol. 10, no. 6, pp. 6552–6565, Nov. 2019.

[18] S. N. Hashemian, M. A. Latify, and G. R. Yousefi, "PEV fast-charging station sizing and placement in coupled transportation-distribution networks considering power line conditioning capability," *IEEE Trans. Smart Grid*, vol. 11, no. 6, pp. 4773–4783, Nov. 2020.

[19] C. Vazquez, F. Iborra, L. Ramirez, H. Sainz, and F. Jurado, "Comparative study of dynamic wireless charging of electric vehicles in motorway, highway and urban stretches," *Energy*, vol. 137, pp. 42–57, Oct. 2017.

[20] H. Ngo, A. Kumar, and S. Mishra, "Optimal positioning of dynamic wireless charging infrastructure in a road network for battery electric vehicles," *Transp. Res. Part D Transp. Environ.*, vol. 85, Aug. 2020, Art. no. 102385.

[21] Z. Bi et al., "Life cycle assessment and tempo-spatial optimization of deploying dynamic wireless charging technology for electric cars," *Transp. Res. Part C Emerg. Technol.*, vol. 100, pp. 53–67, Mar. 2019.

[22] F. Xia, H. Chen, M. Shahidehpour, W. Gan, M. Yan, and L. Chen, "Distributed expansion planning of electric vehicle dynamic wireless charging system in coupled power-traffic networks," *IEEE Trans. Smart Grid*, vol. 12, no. 4, pp. 3326–3338, Jul. 2021.

[23] J. Yang, Y. Xu, and Z. Yang, "Regulating the collective charging load of electric taxi fleet via real-time pricing," *IEEE Trans. Power Syst.*, vol. 32, no. 5, pp. 3694–3703, Sep. 2017.

[24] W. Lee, R. Schober, and V. Wong, "An analysis of price competition in heterogeneous electric vehicle charging stations," *IEEE Trans. Smart Grid*, vol. 10, no. 4, pp. 3990–4002, Jul. 2019.

[25] G. Mouli, M. Kefayati, R. Baldick, and P. Bauer, "Integrated PV charging of EV fleet based on energy prices, V2G, and offer of reserves," *IEEE Trans. Power Syst.*, vol. 10, no. 2, pp. 1313–1325, Mar. 2019.

[26] C. Luo, Y. Huang, and V. Gupta, "Stochastic dynamic pricing for EV charging stations with renewable integration and energy storage," *IEEE Trans. Smart Grid*, vol. 9, no. 2, pp. 1494–1505, Mar. 2018.

[27] B. Zeng and Y. An, "Solving bilevel mixed integer program by reformulations and decomposition," Dept. Ind. Manag. Syst. Eng., Univ. South Florida, Tampa, FL, USA, 2014. [Online]. Available: https://optimization-online.org/2014/07/4455/

[28] H. Zhang, Z. Hu, Z. Xu, and Y. Song, "Optimal planning of PEV charging station with single output multiple cables charging spots," *IEEE Trans. Smart Grid*, vol. 8, no. 5, pp. 2119–2128, Sep. 2017.

[29] M. Shaaban, S. Mohamed, M. Ismail, K. Qaraqe, and E. Serpedin, "Joint planning of smart EV charging stations and DGs in eco-friendly remote hybrid microgrids," *IEEE Trans. Smart Grid*, vol. 10, no. 5, pp. 5819–5830, Sep. 2019.

[30] H. Zhang, S. Moura, Z. Hu, and Y. Song, "PEV fast-charging station siting and sizing on coupled transportation and power networks," *IEEE Trans. Smart Grid*, vol. 9, no. 4, pp. 2595–2605, Jul. 2018.

[31] Z. Liu and Z. Song, "Robust planning of dynamic wireless charging infrastructure for battery electric buses," *Transp. Res. Part C Emerg. Technol.*, vol. 83, pp. 77–103, Oct. 2017.

[32] S. Lv, Z. Wei, G. Sun, S. Chen, and H. Zang, "Optimal power and semi-dynamic traffic flow in urban electrified transportation networks," *IEEE Trans. Smart Grid*, vol. 11, no. 3, pp. 1854–1865, May 2020.

[33] A. Caprara and M. Locatelli, "Global optimization problems and domain reduction strategies," *Math. Program*, vol. 125, no. 1, pp. 123–137, Sep. 2010.

[34] C. Liu, X. Wang, X. Wu, and J. Guo, "Economic scheduling model of microgrid considering the lifetime of batteries," *IET Gener. Transm. Distrib.*, vol. 11, no. 3, pp. 759–767, Feb. 2017.

[35] J. Tan and L. Wang, "Real-time charging navigation of electric vehicles to fast charging stations: A hierarchical game approach," *IEEE Trans. Smart Grid*, vol. 8, no. 2, pp. 846–856, Mar. 2017.

[36] F. Wu, J. Yang, X. Zhan, S. Liao, and J. Xu, "The online charging and discharging scheduling potential of electric vehicles considering the uncertain responses of users," *IEEE Trans. Power Syst.*, vol. 36, no. 3, pp. 1794–1806, May 2021.

[37] X. Zhang, F. Fang, and J. Liu, "Weather-classification-MARS-based photovoltaic power forecasting for energy imbalance market," *IEEE Trans. Ind. Electron.*, vol. 66, no. 1, pp. 8692–8702, Nov. 2019.

[38] "Historical weather data. China meteorological administration (CMA)." [Online]. Available: http://lishi.tianqi.com/wuhan.html AQ2

[39] H. Xu, H. Sun, D. Nikovski, S. Kitamura, K. Mori, and H. Hashimoto, "Deep reinforcement learning for joint bidding and pricing of load serving entity," *IEEE Trans. Smart Grid*, vol. 10, no. 6, pp. 6366–6375, Nov. 2019.

[40] J. Liu, M. G. Lin, S. Huang, Y. Zhou, C. Rehtanz, and Y. Li, "Collaborative EV routing and charging scheduling with power distribution and traffic networks interaction," *IEEE Trans. Power Syst.*, vol. 37, no. 5, pp. 3923–3936, Sep. 2022.

[41] "Beijing requires new parking lots to have vehicle charging piles." [Online]. Available: https://www.yicaiglobal.com/news/beijing-requires-new-parking-lots-to-have-vehicle-charging-piles

[42] "Brussels mandates all car parks to get charging stations by 2025." [Online]. Available: https://www.themayor.eu/en/a/view/brussels-mandates-all-car-parks-to-get-charging-stations-by-2025–11073

[43] W. Gan et al., "Coordinated planning of transportation and electric power networks with the proliferation of electric vehicles," *IEEE Trans. Smart Grid*, vol. 11, no. 5, pp. 4005–4016, Sep. 2020.

[44] Y. Wan, J. Qin, F. Li, X. Yu, and Y. Kang, "Game theoretic-based distributed charging strategy for PEVs in a smart charging station," *IEEE Trans. Smart Grid*, vol. 12, no. 1, pp. 538–547, Jan. 2021.

[45] N. Aguiar, A. Dubey, and V. Gupta, "Network-constrained Stackelberg game for pricing demand flexibility in power distribution systems," *IEEE Trans. Smart Grid*, vol. 12, no. 5, pp. 4049–4058, Sep. 2021.

[46] T. Zhao, Y. Li, X. Pan, P. Wang, and J. Zhang, "Real-time optimal energy and reserve management of electric vehicle fast charging station: hierarchical game approach," *IEEE Trans. Smart Grid*, vol. 9, no. 5, pp. 4049–4058, Sep. 2018.

[47] H. Zhang, Z. Hu, Z. Xu, and Y. Song, "An integrated planning framework for different types of PEV charging facilities in urban area," *IEEE Trans. Smart Grid*, vol. 7, no. 5, pp. 2273–2284, Sep. 2016.

[48] T. Qian, C. Shao, X. Wang, and M. Shahidehpour, "Deep reinforcement learning for EV charging navigation by coordinating smart grid and intelligent transportation system," *IEEE Trans. Smart Grid*, vol. 11, no. 2, pp. 1714–1723, Mar. 2020.

[49] X. Shi, Y. Xu, Q. Guo, H. Sun, and W. Gu, "A distributed EV navigation strategy considering the interaction between power system and traffic network," *IEEE Trans. Smart Grid*, vol. 11, no. 4, pp. 3545–3557, Jul. 2020.